

ORIGINAL ARTICLE

Population pharmacokinetic analysis of RO5459072, a low water-soluble drug exhibiting complex food–drug interactions

Nicole A. Kratochwil¹  | Cordula Stillhart¹ | Cheikh Diack¹ | Sandra Nagel¹ |
Nada Al Kotbi² | Nicolas Frey¹

¹Clinical Pharmacology, Pharmaceutical Research and Early Development, Roche Innovation Center Basel, Roche Holding AG, Switzerland

²PRA Health Sciences, Groningen, Netherlands

Correspondence

Nicole A. Kratochwil, Roche Innovation Center Basel, Bldg. 001/07, CH-4070 Basel, Switzerland.

Email: nicole_a.kratochwil@roche.com

Funding information

Roche Holding AG, Basel, Switzerland

Aims: RO5459072, a cathepsin-S inhibitor, Biopharmaceutics Classification System class 2 and P-glycoprotein substrate, exhibited complex, nonlinear pharmacokinetics (PK) while fasted that seemed to impact both the absorption and the disposition phases. When given with food, all nonlinearities disappeared. Physiologically based PK (PBPK) modelling attributed those nonlinearities to dose-dependent solubilisation and colonic absorption. The objective of this population PK analysis was to complement the PBPK analysis.

Methods: PK profiles in 39 healthy volunteers after first oral dosing (1–600 mg) while fasted or fed in single and multiple ascending dose studies were analysed using population compartmental modelling.

Results: The PK of RO5459072 while fed was characterized by a 1-compartmental PK model with linear absorption and elimination. The nonlinearities while fasted were captured using dose dependent bioavailability and 2 sequential first-order absorption phases: one following drug administration and one occurring 11 hours later and only for doses >10 mg. The bioavailability in the first absorption phase increased between 1 and 10 mg and then decreased with dose, in agreement with in vitro dissolution and solubility studies. The remaining fraction of doses to be absorbed by the second absorption phase was found to have a bioavailability similar to that in the first absorption phase.

Conclusion: The population PK model supported that dissolution- and solubility-limited absorption from the proximal and distal intestine alone explains the nonlinear PK of RO5459072 in fasted state and the linear PK in fed state. This work, together with the PBPK analysis, raised our confidence in the understanding of this complex PK.

Abbreviations: BCS, Biopharmaceutics Classification System; BDDCS, Biopharmaceutics Drug Disposition Classification System; BID, twice daily; CL/F, apparent total clearance; F_{FaDI} , apparent bioavailability of the distal intestine; F_{FaPI} , apparent bioavailability of the proximal intestine; IIV, interindividual variability; LLOQ, lower limit of quantification; MAD, multiple ascending dose; OD, once daily; P-gp, P-glycoprotein (MDR1, multidrug resistance protein 1); PK, pharmacokinetics; SAD, single ascending dose; VPC, visual predictive check.

The authors confirm that the Principal Investigator for this paper is Nada Al Kotbi and that she had direct clinical responsibility for patients. (Nada Al Kotbi M.D., DPM [ULB], Clinical Pharmacologist, Sr. Research physician, Early development service; Van Swietenlaan 6, 9728 NZ Groningen, The Netherlands, alkotbinada@prahs.com, DIRECT: +31 50 40 22 326 • FAX: +31 50 40 22 622 • MOBILE: +31 651707269).

Clinicaltrials.gov, identifiers NCT02295332 (SAD), NCT02521610 (MAD).

This is an open access article under the terms of the Creative Commons Attribution-NonCommercial-NoDerivs License, which permits use and distribution in any medium, provided the original work is properly cited, the use is non-commercial and no modifications or adaptations are made.

© 2021 The Authors. *British Journal of Clinical Pharmacology* published by John Wiley & Sons Ltd on behalf of British Pharmacological Society.

KEYWORDS

pharmacometrics, food-drug interactions, nonlinear pharmacokinetics, low water-soluble drugs

1 | INTRODUCTION

To understand oral absorption of poorly water-soluble drugs is very challenging as it is a complex interplay between the gastrointestinal tract, the dosage form and the active drug species. Significant research efforts are directed towards the improved prediction of absorption for this important drug class^{1,2} by developing advanced in vitro and modelling tools. Sophisticated in vitro tools aim to predict the intraluminal dynamics of the different drug states such as molecularly dissolved, permeable drug and particulate states, e.g. crystalline and amorphous precipitate.¹ New in vivo techniques focus on the physiology of the different gastrointestinal regions and their impact on drug absorption. Gastrointestinal drug disposition studies have shown that the majority of drugs are absorbed in the upper gastrointestinal tract (duodenum and proximal jejunum) mainly due to the higher volume of fluids. Poorly water-soluble drugs have usually prolonged absorption that could lead to absorption from the lower small intestine (distal ileum) as well as from the colon.³⁻⁶ Furthermore, intake of food modulates the regiospecific gastrointestinal physiology leading to potential changes in drug absorption between fasted and fed states.⁷ Pharmacokinetic (PK) food-drug interactions can be driven by 1 or multiple food-specific or unspecific mechanisms, including changes in gastrointestinal lumen conditions (e.g. bile salts concentration, pH, motility), permeation properties (e.g. transporters and metabolizing enzymes), distribution (e.g. lymphatic uptake), as well as metabolism and elimination.⁷ For poorly water-soluble drugs, meal consumption generally facilitates drug dissolution and absorption in the upper gastrointestinal tract due to the increased concentration of lipophilic components, such as food-derived lipids and endogenous bile salts.⁷ An increase in exposure while fed may be beneficial for drug efficacy, but could also represent a potential safety risk.⁸ To understand the absorption mechanisms quantitatively, advanced modelling and simulation techniques and especially physiologically based PK (PBPK) approaches are employed to integrate the in vitro and in vivo data with the aim to optimize clinical formulations in drug research and development.^{9,10}

More empirical compartmental PK models combined with population approaches could also contribute to the understanding of complexity in PK behaviours and provide opportunities to complement the PBPK approach. The work outlined in this paper, directly illustrating this statement, attempts to quantify the nonlinear PK of a **cathepsin-S** (Alexander *et al.* 2019) inhibitor (**RO5459072**) evaluated for the treatment of immune-mediated diseases. RO5459072 belongs to the Biopharmaceutics Classification System (BCS)/Biopharmaceutics Drug Disposition Classification System (BDDCS) class 2 (^{11,12} see Figure S1), being a poorly water-soluble

What is already known about this subject

- Poorly water-soluble drugs can exhibit complex nonlinear pharmacokinetics (PK) during clinical drug development due to the complex interplay between the physiology of the gastrointestinal tract and the physicochemical properties of the drug and the formulation.
- Specific mechanisms such as dissolution- or solubility-limited absorption or the involvement of active drug transport may be the causes of these nonlinear behaviours.
- Mathematical modelling, such as physiologically based PK and compartmental PK analyses, can be applied, even if sometimes challenging, to investigate different hypotheses regarding the underlying mechanism.

What this study adds

- RO5459072, a cathepsin-S inhibitor evaluated for the treatment of immune-mediated diseases and classified as Biopharmaceutics Classification System class 2 drug, exhibited complex nonlinear PK in human under fasted conditions. Mathematical modelling of the PK data was applied to better understand the nonlinear mechanism.
- The presented compartmental PK analysis describes accurately the nonlinearities by including a limited absorption capacity from both the proximal and distal intestines in the fasted state, and an absorption nonlimited and only from the proximal intestine in the fed state.
- These findings confirmed the results of a physiologically based PK analysis, which suggested that dissolution and solubility-limited absorption of RO5459072 could explain the nonlinearity.
- Thus, the compartmental PK modelling approach aligned with the physicochemical characteristics of RO5459072 increased the confidence in the understanding of the complex PK nonlinearity exhibited in fasted state.

and highly permeable drug.¹³⁻¹⁸ It is a dual cytochrome P450-3A and **P-glycoprotein (P-gp)** substrate (Alexander *et al.* 2019) and showed complex nonlinear PK in phase I studies. In the first-in-human single ascending-dose (SAD) study,¹⁸ nonlinearity were

observed in the time concentration profiles of RO5459072 while fasted that seems to impact both the absorption phase and the apparent disposition phase. These nonlinearities disappeared while fed. The presented modelling work shows that the food effect on RO5459072 PK can be accurately described by a compartmental PK model by including a complex absorption step with drug uptake from the proximal and distal intestine in the fasted state, and absorption from the proximal intestine only in the fed state. These findings are in line with the mechanistic understanding of RO5459072 absorption. Thus, the compartmental modelling approach increased our confidence to understand this complex PK behaviour.

2 | METHODS

2.1 | Clinical study conduct

RO5459072, evaluated in clinical trials for the treatment of immune-mediated diseases, was provided by Roche Holding AG, Basel, Switzerland. It is a competitive inhibitor of the active site of cathepsin-S and whose nitrile function allows covalent reversible inhibition to cathepsin-S. For both the first entry into human SAD study and the multiple ascending-dose (MAD) study, healthy volunteers were recruited from PRA Health Sciences, University Medical Center Groningen Groningen, Netherlands. These studies were conducted in accordance with the Declaration of Helsinki, current International Conference on Harmonisation of Technical Requirements for Registration of Pharmaceuticals for Human Use (ICH) guidelines, and all applicable regulatory and ethical requirements. Written informed consent was obtained from all volunteers. The study protocols were approved by Dutch ethics committee (Clinicaltrials.gov, identifiers NCT02295332 [SAD], NCT02521610 [MAD]). The first-in-human SAD study was a single centre, randomized, double-blind, placebo-controlled study to evaluate the PK, pharmacodynamic effects, safety and tolerability of single doses of RO5459072 in healthy male and female volunteers after oral administration under fasted conditions across the dose range of 1 to 600 mg (e.g. single doses of 1, 3, 30, 100, 300 or 600 mg in fasted condition or 100 mg in fed condition—a high-level study design of the SAD study is given in Table S1). A single 1 mg dose was anticipated to produce minimal pharmacological effects, and was therefore consistent with a *minimal anticipated biological effect level* approach to dose selection for entry into human studies. The dose levels after a starting dose of 1 mg were selected in an adaptive manner during study conduct. The study employed an interleaved cohort (*leapfrog*) design. Subjects were recruited in 2 cohorts (cohorts A and B). Four treatment periods were planned for each cohort and individual subjects were randomized to receive a single oral dose of either RO5459072 or placebo in each of the 4 treatment periods with a minimum of 14 days between each study drug administration. Up to 17 subjects were sequentially enrolled in 1 of the 2 cohorts, 15 received 3 doses of RO5459072 (single doses of 1, 3, 10, 30, 100, 300 or 600 mg) and 1 dose of placebo. One subject received 1 dose of 3 mg RO5459072 and 1 dose of

placebo before withdrawing from the study. One subject received 2 doses of RO5459072 (single doses of 100 and 300 mg). Blood samples for PK analyses were taken at 0.5, 1, 2, 3, 4, 5, 6, 8, 10, 12, 24, 36 and 48 h after dosing. All 17 subjects were assessed for safety and tolerability before and after study treatment administration and at various time points during the study. Overall, RO5459072 was similarly tolerated to placebo when administered to healthy volunteers in a single oral dose up to 600 mg.

The study drug was administered as drug in capsule formulation under fasted conditions (overnight fast of at least 8 h). The formulation was an immediate-release dosage consisting of the pure, micronized drug substance filled into size 0 hard-gelatin capsules without additional excipients (dose strengths: 1, 5 and 50 mg). The capsule shell disintegrated rapidly (<10 min) and released the drug substance which showed good wettability in simulated gastric fluids. To assess the effect of food on the PK of RO5459072, a 100-mg dose level was administered following the ingestion of a high-fat high-calorie breakfast. The dose of 100 mg was selected as this dose was expected to be the therapeutic dose producing 1/5 of the no-observed-adverse-effect level exposure in the most sensitive toxicology species and achieving about 97% inhibition of cathepsin-S enzyme activity in average throughout the dosing interval.

The MAD study investigated the PK, the pharmacodynamic effects, the safety and tolerability of RO5459072 after repeat-dose administration to healthy male and female subjects. This multiple-dose study for RO5459072 was a single-centre, randomized, double-blind, placebo-controlled, ascending-dose design study with adaptive dose selection based on safety information (a high-level study design of the MAD study is given in Table S2). Treatment was given with food. The oral dose levels were 50, 100 or 200 mg of RO5459072 or placebo. The dose of 100 mg (97% inhibition of cathepsin-S enzyme activity) had been very well tolerated in the SAD study and was selected for as the starting dose as it was anticipated to be the therapeutic dose. A lower dose of 50 mg was also explored achieving about 93% inhibition of cathepsin-S enzyme activity in average throughout the dosing interval. On day 1, the subjects received 1 dose and on day 3 up to day 9 they received either a twice daily (BID) or a once daily (OD; only for 100 mg) dosing. Twenty-two subjects were sequentially enrolled in 1 of 4 cohorts with the following dosing regimens 100 mg BID, 50 mg BID, 100 mg OD and 200 mg BID. In each cohort, subjects received OD or BID oral doses of RO5459072 or placebo with treatments assigned in a 6:3 ratio. In the 200-mg BID cohort (following withdrawal of consent prior to Day 1 for 3 subjects) of 6 subjects, 4 subjects received active treatment and 2 subjects received placebo. Intensive PK samples were collected up to 48 h after the first dose and before the second dose (i.e.: 0.5, 1, 2, 3, 4, 5, 6, 8, 10, 12, 24, 36 and 48 h) and similarly after the last dose on day 9 but only up to 24 h postdose. Additional PK samples were collected every day from day 4 to day 9 just before the morning dose. All 22 subjects were assessed for safety and tolerability before and after study treatment administration and at various time points during the study. Overall, RO5459072 doses up to 200 mg BID for 7 days were tolerated similarly to placebo by healthy volunteers.

2.2 | Bioanalysis

The concentrations of RO5459072 in human plasma containing tripotassium ethylenediaminetetraacetic acid as an anticoagulant were determined using liquid–liquid extraction followed by liquid chromatography with tandem mass spectrometric detection. The analytical method was validated and found to be suitable for the determination of RO5459072 in human plasma over the calibration range of 1.00–1000 ng/mL. The precision (relative standard deviation % relative standard deviation) values were $\leq 15.0\%$ ($\leq 20.0\%$ at the lower limit of quantification [LLOQ] of 1 ng/mL) and the accuracy (mean %) values were within $\pm 15.0\%$ ($\pm 20.0\%$ at the LLOQ) of the nominal concentration for each quality control concentration within each analytical run (intra-assay) and between runs (inter-assay).

2.3 | Dataset

To investigate the complex nonlinearities following single administration in fasted-state, a dataset was built with the PK plasma concentrations collected after the first dose administration, either fasted or fed, in the SAD and MAD studies. In total, the dataset was composed of 816 RO5459072 plasma concentration from 39 healthy male and female subjects (17 subjects from the SAD and 22 subjects from the MAD study).

2.4 | PK model development

Population PK analyses of the drug concentration data were performed using NONMEM 7.3 (ICON Development Solutions, Hanover, MD). R (version 3.1.0, rproject.org) was employed for data management, graphical analysis and standard statistical analysis. For model management and NONMEM output visualization, Pirana (version 2.9.2) was used. The model development was done with the ADVAN9 subroutine and the first-order conditional estimation method. For the final disposition model selection, 1- and 2-compartment models were tested. First-order input with or without a lag time, different transit compartments were tested for the absorption. In addition, individual bioavailability parameters for each dose were estimated at the beginning of the absorption modelling in order to derive the mathematical equations for the proximal and distal absorption and their relationship. Interindividual variability (IIV) was evaluated for each model parameter and was modelled using a log-normal distribution. No interoccasion variability (IOV) was estimated and each period in the cross-over design of the SAD study was considered as a different subject. This was done to limit the complexity of the analysis by avoiding a potential increase in the residual variability and by limiting the number of parameters to be estimated. However, to confirm that they were no occasion effect, ETAs IOV were derived by computing the delta between the average ETAs across occasions and the ETA at a given occasion for each individual. The ETAs IOV were graphically compared between

periods and the coefficient of variation of the delta per parameter represent the IOV of the parameter.

Different error models (proportional, additive, combined proportional–additive and time dependent) were evaluated for the residual variability. Change in objective function value (i.e. drop of 3.84 for 1 parameter; $P = .05$), diagnostic plots and parameter estimate precisions were used to discriminate between the models. Beside the food effect, the potential effects of demographic covariates on the PK of RO5459072 were only investigated graphically and not in this population PK analysis as the subjects were all healthy volunteers with a rather narrow range of covariates.

2.5 | Model qualification

The goodness of fit of all models was determined by observation vs. population and individual prediction plots. For examination of the prediction performance of the models, visual predictive checks (VPCs) were run by means of Perl-Speaks-NONMEM (PsN) with 500 simulations using the final parameter estimates.

2.6 | Nomenclature of targets and ligands

Nomenclature of Targets and Ligands Key protein targets and ligands in this article are hyperlinked to corresponding entries in <http://www.guidetopharmacology.org>, and are permanently archived in the Concise Guide to PHARMACOLOGY 2019/20.^{30,31}

3 | RESULTS

3.1 | PK observations

For the PK assessment of the BCS 2 class RO5459072, a small molecule inhibitor of cathepsin-S, 39 healthy male and female subjects (17 subjects from the SAD and 22 subjects from the MAD study) provided 816 plasma concentration values from intensive sampling after a first, oral administration in fasted and fed conditions (10% of these data were below the LLOQ of 1 ng/mL and they were not retained in this analysis). The time–concentration profiles of RO5459072 are shown in Figure 1A and B for oral doses of 1–600 mg while fasted. The increase in systemic exposure of RO5459072 is more than dose proportional for doses <10 mg and less than dose proportional for doses >30 mg as shown in the dose normalized concentration–time profiles of RO5459072 in Figure 1A and in the noncompartmental analysis parameters provided in Table S3. The noncompartmental analysis apparent terminal half-life increased from approximately 8 hours at the 10 mg dose to approximately 13–16 hours at the highest doses between 100 and 600 mg (Figure 1B, Table S3).

Contrary to the fasted state, the PK of RO5459072 was linear under fed condition from 50 to 100 mg as shown by the dose normalized plasma concentration time profiles in Figure S2. Comparing

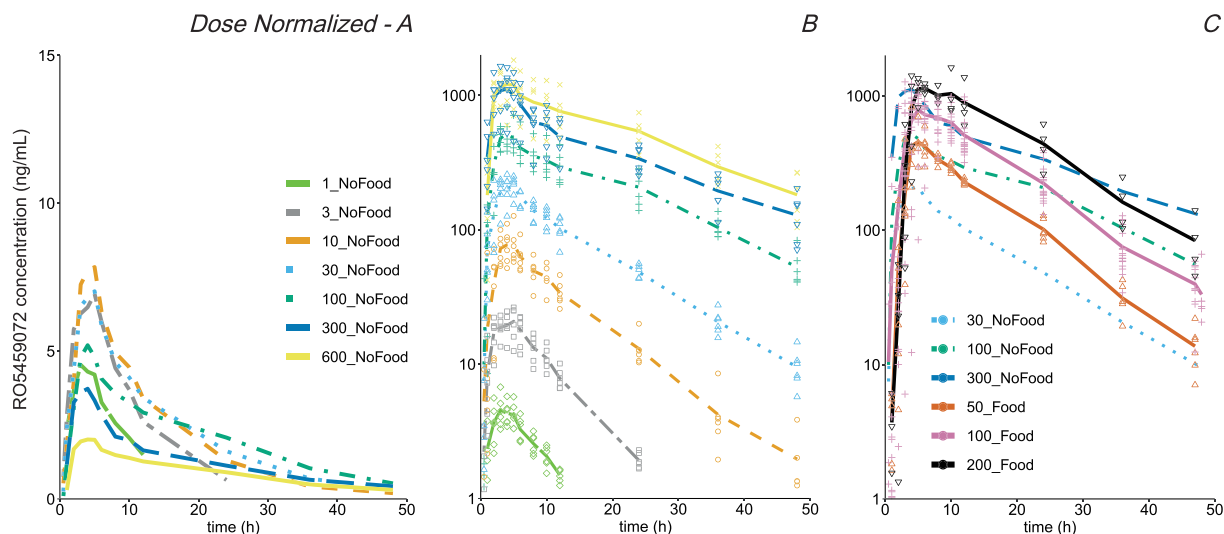


FIGURE 1 Observed time–concentration profiles of RO5459072 in healthy volunteers while fasted or fed across the dose range of 1 to 600 mg. (A, B) After a single oral dose between 1 and 600 mg while fasted. (A) Dose normalized time–concentration profiles show nonlinearity in the absorption phase (symbols show the individual data, lines present observed average). (B) Nonlinearity in the apparent disposition phase of RO5459072 can be observed. Symbols present doses of 1 mg (light green diamonds, very long-dashed line), 3 mg (grey square, long-dashed dotted line), 10 mg (ochre circle, short-dashed line), 30 mg (light blue upper triangle, dotted line), 100 mg (green cross, short-dashed dotted line), 300 mg (dark blue lower triangle, long-dashed line), 600 mg (yellow x, solid line). (C) Comparison of 30 mg, 100 mg and 300 mg doses under fasted conditions and 50 mg (brown upper triangle, solid line), 100 mg (rose cross, solid line) and 200 mg (black lower triangle, solid line) doses under fed conditions. Food increased the extent of absorption and the T_{max} value, but decreased the estimated average half-life using noncompartmental analysis by approximately 4 hours

fasted (30 mg, 100 mg and 300 mg doses) and fed conditions (50 mg, 100 mg and 200 mg doses) in the semilogarithmic graph, showed the strong influence of food intake on the time concentration profiles of RO5459072 (Figure 1C, Tables S4 and S5). The absorption phase while fed was slightly longer giving rise to a T_{max} -value of 5 hours, which was approximately 1 hour later as at fasted condition and at 100 mg, an increase in the RO5459072 exposure was observed as compared to the fasted state. Furthermore, unexpectedly, the average estimated terminal half-lives in fed states were faster as compared to fasted states and similar across all studied doses (50 mg, 100 mg, 200 mg dose) ranging between 8–10 hours (Figure 1C, Tables S4 and S5). Thus, food intake changed the PK of RO5459072.

3.2 | Population PK model

The objective of the presented compartmental PK modelling approach was to quantify the nonlinear PK of RO5459072, observed under fasted condition, in alignment with the mechanistic understanding of RO5459072 absorption.

The final compartmental PK model describes the PK data of RO5459072 in fasted (doses from 1 to 600 mg) and fed conditions (doses from 50 to 200 mg) after the first oral administration. The model scheme is presented in Figure 2A.

In the fasted state, the absorption phase was modelled by 2 sequential first-order absorption processes. The first had 3 transit compartments representing the absorption from the proximal

segments of the intestine (i.e. duodenum and proximal jejunum) and the second had a lag time of 11.2 h representing the absorption from the distal segments of the intestine (i.e. distal ileum and colon). For the 2 lowest doses of 1 and 3 mg, no distal absorption was needed and the apparent bioavailabilities of the proximal intestine (F_{FaPI}) were estimated to be 0.49 and 0.74, respectively. For doses >10 mg, the F_{FaPI} values were found to decrease with dose following a maximum effect (E_{max}) function and the apparent bioavailability of the distal intestine (F_{FaDI}) was found to be equal to the product of F_{FaPI} with the fraction of dose that was not absorbed in the proximal intestine, as described by the following equations:

$$F_{FaPI} = 1 - \frac{(D - D_{10mg})}{(D - D_{10mg}) + (D_{50} - D_{10mg})} \quad (1)$$

$$F_{FaDI} = F_{FaPI} * (1 - F_{FaPI}) \quad (2)$$

The dose of 10 mg was used as a reference for F_{FaPI} as this dose had the maximal dose-normalized exposure. For doses between 10 and 600 mg, F_{FaPI} (Equation 1) was found to decrease with dose from 1 to 0.26 with an E_{max} of 1 and a D_{50} -value of 216 mg. As a result, F_{FaDI} (Equation 2) increased initially with dose up to 0.25 at around 100 mg and then declined slowly with increasing doses. Figure 2B shows the estimated F_{FaPI} and F_{FaDI} values in fasted state vs. dose. In addition, the total apparent bioavailability (F_a) in fasted state is displayed in Figure 2B, which is the sum of F_{FaPI} and F_{FaDI} , and is decreasing from 1 to 0.5 when the dose increases from 10 to 600 mg.

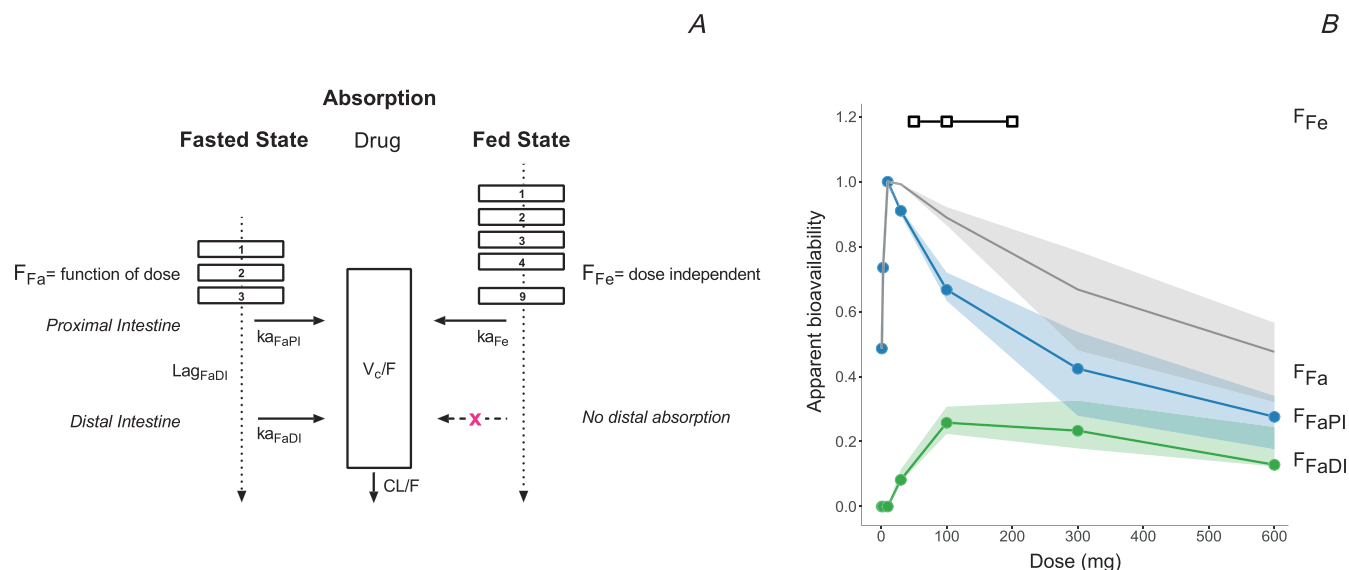


FIGURE 2 Population pharmacokinetic model for RO5459072. (A) Model scheme (B) Model-derived relative values of apparent bioavailability vs. dose in fasted and fed states. Lines present the median of the bioavailability with 95% confidence intervals (shadowed areas). Solubility-limited absorption from the proximal and distal intestine explains the nonlinear pharmacokinetics of RO5459072 while fasted, which disappeared while fed. CL/F , apparent total clearance; F_{FaPI} (Equation 1), apparent bioavailability of the proximal intestine while fasted which is modelled as E_{max} function of dose where D_{50} is defined as dose where 50% of the maximal bioavailability is reached, which was set arbitrarily to 1 for a dose of 10 mg; F_{FaDI} (Equation 2), apparent bioavailability of the distal intestine while fasted, which is a function of F_{FaPI} . F_{Fa} is the total bioavailability in fasted state being the sum of the apparent bioavailability of the proximal and distal intestine, F_{FaPI} and F_{FaDI} , respectively; F_{Fe} , apparent bioavailability in fed condition, which is independent of dose; k_{aFaPI} , first-order absorption rate constant of the proximal intestine in fasted condition; Lag_{FaDI} , lag time for the distal intestine absorption; k_{aFaDI} , first-order absorption rate constant of the distal intestine in fasted condition, k_{aFe} , first-order absorption rate constant in fed condition; V_c/F , apparent central volume of distribution

The absorption rate was estimated to be 2.95 h^{-1} for both doses of 1 and 3 mg. For doses between 10 and 600 mg, the first-order absorption rates from the proximal and distal intestine were estimated to be 2.05 h^{-1} and 0.065 h^{-1} , respectively. The value of 0.065 h^{-1} translates into $t_{1/2}$ of 10.6 h for the absorption from the distal intestine.

For the fed condition (50 mg, 100 mg and 200 mg doses), the absorption phase was modelled by a first-order absorption rate with 9 transit compartments. The transit compartments were included sequentially until no significant model improvement was observed. No absorption from the distal intestine could be estimated indicating complete absorption from the proximal intestine. The apparent bioavailability was dose independent and was estimated to be 18% higher than the apparent bioavailability fixed to 1 for the reference dose of 10 mg in the fasted state (see Figure 2B). The absorption rate in fed state was 2.95 h^{-1} (same as for doses of 1 and 3 mg in fasted state).

Disposition was described for fasted (1–600 mg dose) and fed conditions (50 mg, 100 mg, 200 mg dose) by a 1-compartment model with linear clearance from the central compartment. The apparent volume (V_c/F) and clearance (CL/F) were estimated to be 109 L and 9.38 L h^{-1} , respectively.

IIVs were implemented using exponential error models on the absorption rates in fasted (for doses between 10 and 600 mg) and fed states, the apparent volume, the apparent clearance, the

D_{50} -value and the apparent bioavailability of the distal intestine (F_{FaDI}). IIVs on additional parameters, such as on F_{FaPI} and total F_{Fa} (sum of F_{FaPI} and F_{FaDI}), were evaluated during the model development, but they did not improve the model further and therefore only the most influential parameters were kept in the final model. Shrinkage for D_{50} and F_{FaDI} was found to be high and around 40% due to limited data.

The graphical explorations of the ETAs IOV and their values are given in Figure S3. The IOVs were found to be small and therefore only slightly inflating the estimated interindividual variability of the parameters.

Residual variability was modelled using 2 proportional error models: one used uniquely for the first 2 hours following oral drug intake in fed conditions; and one used for the rest of the data.

The diagnostic plots of the final model for all doses in fasted and fed state showed no apparent bias. In Table 1, the population PK estimates are given.

The VPCs (Figure 3A,B) and the prediction corrected (pc)VPCs (Figure 3C,D) for fasted (Figure 3A,C) and fed states (Figure 3B,D, additional VPCs for each dose can be found in Figure S4) demonstrate good overall performance of the model. The model described well the single-dose PK data in fasted (Figure 3A,C) and fed conditions (Figure 3B,D). The lower panels of the pcVPC in Figure 3C and D show the simulation based 95% confidence intervals around the median for the fraction of LLOQ values and its agreement with the fraction LLOQ

TABLE 1 Final population pharmacokinetic estimates

Parameters (units)	Estimates (% RSE)
Fasted condition	
k_{aFaPI} (h^{-1}) for doses > 3 mg	2.05 (6.29)
D_{50} (mg)	216 (13.4)
k_{aFaDI} (h^{-1}) for doses > 3 mg	0.065 (9.31)
Lag_{FaDI} (h) for doses > 3 mg	11.2 (6.92)
F_{FaPI} for a dose of 1 mg	0.486 (8.77)
F_{FaPI} for a dose of 3 mg	0.735 (7.85)
Fed condition	
F_{Fe}	1.18 (4.70)
Fasted and fed conditions	
CL/F ($L h^{-1}$)	9.38 (3.65)
V_c/F (L)	109 (4.76)
k_{aFa} (h^{-1}) for doses of 1 and 3 mg while fasted and k_{aFe} (h^{-1}) while fed	2.95 (3.12)
IIV	
	CV% (% RSE) [*]
CL/F	13.1% (12.0) [21.7%]
V_c/F	24.0% (15.0) [14.6%]
k_{aFaPI} for doses > 3 mg	33.8% (13.8) [2.44%]
k_{aFe}	39.2% (14.8) [4.21%]
F_{FaDI}	32.1% (38.9) [41.0%]
D50	38.5% (27.3) [40.9%]
Residual errors	
Proportional (fasted and time after first dose > 2 hr in fed condition)	24.4% (2.97%)
Proportional (time after first dose \leq 2 hr in fed condition)	199% (1.19%)

* η - shrinkages are indicated in brackets. Data are population means and relative standard errors (RSE); interindividual (IIV) and residual variability are presented as coefficient of variation (CV%). CL/F, apparent total clearance; F_{FaPI} (Equation 1), apparent bioavailability of the proximal intestine while fasted which is modelled as E_{max} function of dose where D_{50} is defined as dose where 50% of the maximal bioavailability is reached, which was set arbitrarily to 1 for a dose of 10 mg; F_{FaDI} (Equation 2), apparent bioavailability of the distal intestine while fasted, which is a function of F_{FaPI} ; F_{Fe} , apparent bioavailability in fed condition, which is independent of dose; k_{aFaPI} , first-order absorption rate constant of the proximal intestine in fasted condition; Lag_{FaDI} , lag time for the distal intestine absorption; k_{aFaDI} , first-order absorption rate constant of the distal intestine in fasted condition; k_{aFe} , first-order absorption rate constant in fed condition; V_c/F , apparent central volume of distribution

samples. Thus, an implementation of the M3 method¹⁹ was not further considered for the final model as the LLOQ observations (LLOQ of 1 ng/mL, 10% of the data) were well predicted and no model bias was detected. Furthermore, the VPC (given in Figure S5) for the 100 mg OD dosing demonstrated the ability of the model to predict multiple-dose data in a prospective setting and showed PK linearity while fed. Only the VPC for the 100 mg OD dose was provided to illustrate the evaluation of the model adequacy in predicting multiples doses because it was the only dosing regimen in the MAD

study where it was known that the food was given close to the drug administration. All the other doses were given twice a day (BID administration) and after day 1, the diners were served without any restrictions on timing relative to study drug administration. Assuming a systematic concomitant administration of the diners and the drug, the VPCs for the BID doses were not as good as for the OD dose indicating that the assumption was not fully correct.

4 | DISCUSSION

The BCS class 2 drug RO5459072, a cathepsin-S inhibitor currently evaluated for the treatment of immune-mediated diseases, exhibited complex nonlinear PK behaviour following oral administration in fasted state in healthy volunteers that seemed to impact both the absorption and the disposition phases. Those nonlinearities disappeared when the drug was given with food. As RO5459072 is poorly water-soluble and a P-gp substrate, there was an initial uncertainty about the underlying mechanisms of the nonlinear PK. Preliminary PBPK absorption modelling combined with in vitro studies suggested that dissolution- and solubility-limited absorption and colonic absorption could explain the observed nonlinearities for RO5459072. The objective of this work was to apply compartmental PK methods using nonlinear mixed effect models to test further the PBPK suggestions.

RO5459072 is a neutral and highly permeable compound. As expected for a BCS/BDDCS 2 class drug, the low solubility (<0.02 mg/mL) translated under fasted conditions into a dose-dependent nonlinearity in the absorption phase in the SAD study (Figure 1A) characterized by a decrease in the apparent bioavailability at doses >10 mg. For the lower doses (1 and 3 mg) while fasted, a decrease in apparent bioavailability was also observed when compared to the 10 mg dose. These nonlinearities can be explained by the dissolution- and solubility-limited absorption of the compound. RO5459072 was administered as a micronized powder in capsule formulation in Phase 1 studies. In vitro dissolution studies in bio-relevant media showed a lower extent of solubilisation than expected based on solubility data at concentrations that are representative for the lowest dose levels, which can explain the lower fraction absorbed. For higher doses, the fraction dissolved in the in vitro experiment exceeded the equilibrium solubility of the crystalline drug resulting in a supersaturated solution. The extent of supersaturation increased slightly with increasing doses and was induced by the partially amorphous (~35% w/w) material generated during the micronization process of the drug substance (jet milling; see Figure S6). Therefore, at higher doses, the solubility-limited absorption of RO5459072 led to a decrease in bioavailability in the dose range from 10 to 600 mg.

Nonlinearity was not only seen in the absorption phase in the SAD study subjects while fasted, but also in the apparent disposition phase (Figure 1B) which was unexpected. The increase in apparent terminal half-life with dose and the shape of the concentration-time curve in the disposition phase suggested first a concentration-dependent elimination process for RO5459072, which appeared to be saturated for

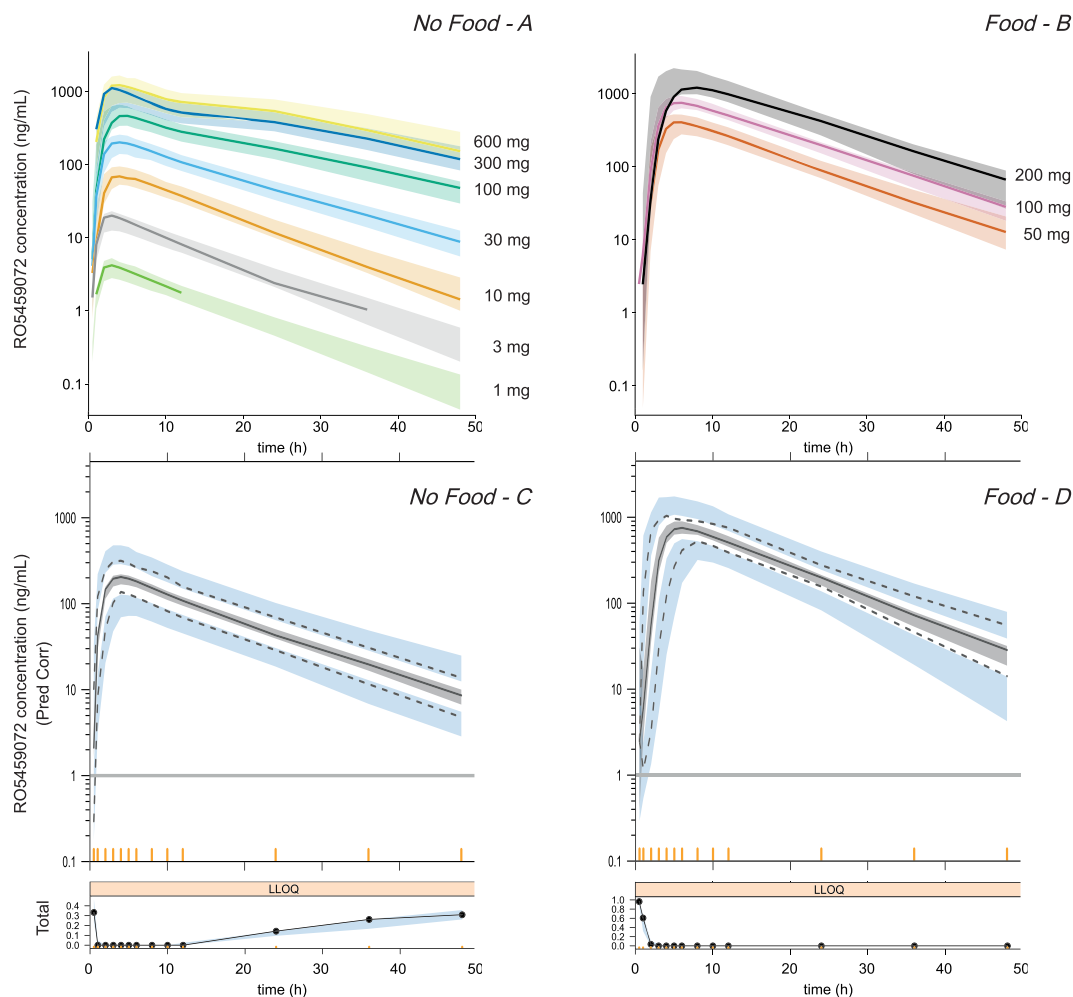


FIGURE 3 Visual predictive checks (VPCs) of the observed medians of the time–concentration profiles of RO5459072 per dose and prediction-corrected VPCs. Time on the x-axis is given since the first dose in hours, with concentrations on the y-axis. Concentrations (A, B) and prediction corrected (C, D) concentrations of RO5459072 after first oral dosing in healthy volunteers (A, C) in fasted states (1 mg, 3 mg, 10 mg, 30 mg, 100 mg, 300 mg and 600 mg dose) or (B, D) in fed states (50 mg, 100 mg and 200 mg dose). For the simulation, the time-dependent residual error before 2 hours in fed condition was not used. (A, B) The median (50th percentiles) of the observations are presented in solid lines. The 95% confidence intervals of the 50th percentiles of the model predictions are presented in shaded areas. (C, D) Percentiles of observations are presented in black, with solid lines for 50th percentiles and dashed lines for 2.5th and 97.5th percentiles. The 95% confidence intervals of the 50th, 2.5th and 97.5th percentiles of the simulated predictions are presented in dark grey and light blue shaded areas, respectively. The lower panels show simulation based 95% confidence intervals (blue areas) around the median for the fraction of lower limit of quantification values. The observed fraction of observed lower limit of quantification samples are represented with a solid line. The model described well the observed time concentration profiles in healthy volunteers while fasted or fed after the first dose across the dose range of 1–600 mg

concentrations above 100 ng/mL. As RO5459072 is a strong P-gp substrate, the initial assumption was that the nonlinearity in the disposition of RO5459072 was due to the involvement of P-gp transporters. Furthermore, in rats, 50% of an intravenous dose was found unchanged in the faeces suggesting direct intestinal secretion by P-gp (data held on files at Roche Holding AG, Basel, Switzerland). Detailed in vitro studies, however, demonstrated that human P-gp was not saturable up to RO5459072 concentrations of 100 μ M (data held on files at Roche Holding AG, Basel, Switzerland). Thus, saturation of P-gp transporters could be ruled out. In addition, follow-up in vitro enzymology studies demonstrated the absence of time-dependent metabolic enzyme inhibition by RO5459072 and its metabolites (data held on files at Roche

Holding AG, Basel, Switzerland). These findings therefore excluded a concentration- or time-dependent clearance for RO5459072 as potential explanations and pointed towards a late absorption phenomenon.

Under fed condition, the dose dependent nonlinearity in the absorption phase disappeared. As predicted for this class, food intake increased significantly the fraction absorbed of RO5459072 by increasing its solubility (Figure 1C). Surprisingly, in the first instance, the apparent disposition phase was linear and faster in fed subjects (Figure 1C). Thus, food changed the PK of RO5459072 when given shortly before drug administration, but not in over-night fasted healthy volunteers, who received food 4 hours after dosing and then regularly thereafter. Only a late absorption phenomenon from the distal

intestine could explain why food influenced the PK of RO5459072 during drug dosing but not thereafter. After oral administration, the drug passes through the stomach (1–2 hours) and small intestine (3–4 hours) before reaching the colon.²⁰ The colonic transit time is 8–35 hours on average before unabsorbed drug is excreted into the faeces.²⁰ This transit time is independent of the gastric emptying rate and the small intestinal transit time and varies significantly between subjects, sexes and studies.^{21–25} Thus, the reported colonic transit time of up to 35 hours supports a late absorption of RO5459072 and could explain the nonlinearity observed in the apparent disposition phase.

To raise our confidence in the understanding of the complex PK and to support later clinical development for RO5459072, a population PK model was built.

In the population PK model, the complex nonlinearities in the fasted state could be well captured using dose-dependent apparent bioavailability and 2 sequential first-order absorption phases combined with a 1-compartment model with linear elimination. The first absorption phase that follows the drug administration was assumed to take place in the proximal intestine and was characterized by a series of 3 transit compartments. The apparent bioavailabilities in this first phase, compared to 10 mg fasted, were of 0.5 and 0.7 for doses of 1 and 3 mg, respectively, and are in line with the slow dissolution rate observed *in vitro* at concentrations below saturation solubility of RO5459072. For doses >10 mg, the proximal bioavailability decreased with dose following an E_{\max} to a value of 0.3 at a dose of 600 mg. The second absorption phase was identified only for doses >10 mg and was found to start a bit more than 11 hours after drug intake following a first-order process and was assumed to take place in the distal intestine.

This long estimated lag time for distal absorption is in line with experimentally observed gastric and small intestinal mean transit times of >6 hours in total before reaching the colon.²⁰ The remaining fraction of doses to be absorbed by the second absorption phase was found to have an apparent bioavailability similar to that in the first absorption phase.

The apparent fraction of the total dose absorbed from the distal intestine was ~16% on average for doses between 10 and 600 mg, which is in agreement with the PBPK absorption modelling estimating 10% of the dose across this dose range. A detailed description of the refined PBPK absorption model and its application for formulation development of this compound will be published elsewhere as it would go beyond the scope of this manuscript. Overall, the apparent total bioavailability in the fasted state decreases from 1 to 0.5 when doses increase from 10 to 600 mg.

In the fed state, only absorption in the proximal intestine was found, and a series of 9 transit compartments was applied to model the delay in absorption with food intake due to changes in gastrointestinal physiology, such as delayed gastric emptying.⁷ The apparent bioavailability in the fed state was found to be dose independent and was estimated to be 20% higher than the apparent bioavailability of the reference dose of 10 mg in the fasted state. The VPCs for the 50 mg, 100 mg and 200 mg doses (Figure S4) showed good prediction for the observed PK data supporting a linear absorption while fed,

even though the observed normalized peak plasma concentrations from a total of 4 patients for a dose of 200 mg seemed to be slightly lower than those achieved for doses of 50 and 100 mg (Figure S2).

For fasted and fed conditions, clearance was linear with an estimated value of 9.38 L h^{-1} from a single compartment.

The derived population PK model showed good overall performance under both fasted and fed conditions as showed by the VPC and pcVPC. (Figure 3A and Figure S4). All fixed effects were estimated with good precision and most of the random effects were estimated with reasonable precision. The main residual error was moderate (24%); however, the time dependent residual error used for the first 2 hours in the fed state was large (199%). The use of a time-dependent error is suggested when the absorption phase is complex and could potentially be less well characterized by the model than the disposition phase.²⁶ It avoids the magnitude of the error in the absorption phase to be propagated to the disposition phase. The impact of this large residual error in the early time under fed conditions was however limited. Indeed, all the VPC and pcVPCs under fed conditions were done without this time-dependent error and they showed that the model is able to simulate properly the full PK profile including the first 2 hours postdose. No multiple dose data were included in the population PK model development as the main objective was to characterize the differences between food and fasted state following the first oral administrations of RO5459072; however, to show the ability of this model to predict the PK of RO5459072 following multiple doses, a VPC of the 100 mg OD dose in the MAD study is provided in Figure S5.

Drug absorption from the lower small intestine (distal ileum) and colon is reported in the literature,²⁷ for example for lumiracoxib⁶ and tacrolimus.⁵ Recently, Heimbach *et al.* reported the PK of the poorly water-soluble, highly permeable BCS class 2 drug NVS406. NVS406 showed constant plasma concentrations between 12 and 48 hours after administration declining rapidly thereafter.²⁸ The authors speculated that this concentration–time profile was due to a prolonged and slow absorption from the colon. Based on oral absorption modelling, they predicted that ~45% of the total dose was absorbed from the colon in the fasted state. In fed state, colonic absorption was diminished to <13% of the total absorbed dose and the main absorption occurred in the proximal intestine due to improved *in vivo* solubility.

The presented work, together with the drug examples in the literature, indicated that colonic absorption can be the reason for nonlinear time–concentration profiles several hours after dosing. As the focus was on immediate-release dosage forms, site of absorption studies using controlled delivery devices have not been conducted with RO5459072 to validate the hypothesis of the late absorption for the nonlinear PK of RO5459072. The use of such strategies would have been very insightful. From a technical perspective, however, the conductance of regional release studies with RO5459072 would be very challenging due to the poor solubility properties of the compound that limits the control of its release profile in the gastrointestinal tract. Aspiration studies would be a potential alternative method for assessing the regional absorption profile. However, in contrast with the situation in the upper gastrointestinal lumen, collection of aspirates from the distal

intestine is problematic, due to the limited and viscous volumes available in the region, as highlighted in a recent review.²⁹ Therefore, the use of indirect methods such as mechanistic absorption modelling is still the most commonly applied method for verifying the regional absorption behaviour of drug candidates.

Finally, it is important to understand the mechanism beyond nonlinear PK before studying relationships between drug exposure and efficacy or safety during clinical development. Thus, the compartmental PK modelling approach in alignment with the mechanistic understanding of RO5459072 absorption increased our confidence to understand this complex PK behaviour.

ACKNOWLEDGEMENTS

The authors thank all the subjects who participated in this study, which was funded by Roche Holding AG, Basel, Switzerland. We thank in addition Christoph Funk, Mohammed Ullah, Stefan De Buck and Neil J. Parrott (Roche Pharmaceutical Research and Early Development, Roche Innovation Center Basel, Basel, Switzerland) for their valuable discussions. We would also like to acknowledge Darren Bentley (former Roche employee, currently at Certara Strategic Consulting, London, UK) for his leading role in the design of the clinical studies, Pawel Dzygiel (Roche Pharmaceutical Research and Early Development, Roche Innovation Center Basel, Basel, Switzerland) for the bioanalytics of the PK samples, and all the people involved at Roche Basel for providing the preclinical and clinical data. The author(s) received no specific funding for this work.

COMPETING INTERESTS

The authors Nicole A. Kratochwil, Cordula Stillhart, Cheikh Diack, Sandra Nagel and Nicolas Frey are employees of Roche Holding AG, Basel, Switzerland. Author Nicolas Frey owns stock in Roche Holding AG.

CONTRIBUTORS

N.A.K., C.S., C.D., S.N., and N.F. wrote the manuscript; S.N. and C.S. performed the research and N.A.K., C.S., C.D. and N.F. analysed the data.

DATA AVAILABILITY STATEMENT

The PK data used and analysed during these clinical studies (Clinicaltrials.gov, identifiers NCT02295332 [SAD], NCT02521610 [MAD]) are included in this published article [and its supplementary files] and are available on reasonable request. For further details on Roche's Global Policy on the Sharing of Clinical Information and how to request access to related clinical study documents, see here (https://www.roche.com/research_and_development/who_we_are_how_we_work/clinical_trials/our_commitment_to_data_sharing.htm).

ORCID

Nicole A. Kratochwil  <https://orcid.org/0000-0002-2149-4375>

REFERENCES

- Boyd BJ, Bergström CAS, Vinarov Z, et al. Successful oral delivery of poorly water-soluble drugs both depends on the intraluminal behavior of drugs and of appropriate advanced drug delivery systems. *Eur J Pharm Sci.* 2019;137:104967. <https://doi.org/10.1016/j.ejps.2019.104967>
- Vertzoni M, Augustijns P, Grimm M, et al. Impact of regional differences along the gastrointestinal tract of healthy adults on oral drug absorption: An UNGAP review. *Eur J Pharm Sci.* 2019;134:153-175. <https://doi.org/10.1016/j.ejps.2019.04.013>
- Fink C, Sun D, Wagner K, et al. Evaluating the role of solubility in oral absorption of poorly water-soluble drugs using physiologically-based pharmacokinetic modeling. *Clin Pharmacol Ther.* 2020;107(3):650-661. <https://doi.org/10.1002/cpt>
- Murakami T. Absorption sites of orally administered drugs in the small intestine. *Expert Opin Drug Discovery.* 2017;12(12):1219-1232. <https://doi.org/10.1080/17460441.2017.1378176>
- Tsunashima D, Kawamura A, Murakami M, et al. Assessment of tacrolimus absorption from the human intestinal tract: open-label, randomized, 4-way crossover study. *Clin Ther.* 2014;36(5):748-759. <https://doi.org/10.1016/j.clinthera.2014.02.021>
- Wilding IR, Connor AL, Carpenter P, et al. Assessment of lumiracoxib bioavailability from targeted sites in the human intestine using remotely activated capsules and gamma scintigraphy. *Pharm Res.* 2004;21(3):443-446.
- Koziolek M, Alcaro S, Augustijns P, et al. The mechanisms of pharmacokinetic food-drug interactions - A perspective from the UNGAP group. *Eur J Pharm Sci.* 2019;134:31-59. <https://doi.org/10.1016/j.ejps.2019.04.003>
- Deng J, Brar SS, Lesko LJ. To take or not to take with meals? Unraveling issues related to food effects labeling for oral antineoplastic drugs. *Clin Pharmacol Drug Dev.* 2018;7(5):455-464. <https://doi.org/10.1002/cpdd.416>
- Parrott N, Lave T. Applications of physiologically based absorption models in drug discovery and development. *Mol Pharm.* 2008;5(5):760-775. <https://doi.org/10.1021/mp8000155>
- Stillhart C, Pepin X, Tistaert C, et al. PBPK absorption modeling: Establishing the in vitro-In vivo link-Industry perspective. *AAPS J.* 2019;21(2):19. <https://doi.org/10.1208/s12248-019-0292-3>
- Benet LZ, Broccatelli F, Oprea TI. BDDCS applied to over 900 drugs. *AAPS J.* 2011;13(4):519-547. <https://doi.org/10.1208/s12248-011-9290-9>
- Benet LZ. The role of BCS (Biopharmaceutics Classification System) and BDDCS (Biopharmaceutics Drug Disposition Classification System) in drug development. *J Pharm Sci.* 2013;102(1):34-42. <https://doi.org/10.1002/jps.23359>
- Baugh M, Black D, Westwood P, et al. Therapeutic dosing of an orally active, selective cathepsin-S inhibitor suppresses disease in models of autoimmunity. *J Autoimmun.* 2011;36(3-4):201-209. <https://doi.org/10.1016/j.jaut.2011.01.003>
- Gupta S, Singh RK, Dastidar S, Ray A. Cysteine cathepsin-S as an immunomodulatory target: present and future trends. *Expert Opin Ther Targets.* 2008;12(3):291-299. <https://doi.org/10.1517/14728222.12.3.291>
- Hargreaves P, Daoudlarian D, Theron M, et al. Differential effects of specific cathepsin-S inhibition in biocompartments from patients with primary Sjögren syndrome. *Arthritis Res Ther.* 2019;21(1):175. <https://doi.org/10.1186/s13075-019-1955-2>
- Hilpert H, Mauser H, Humm R, et al. Identification of potent and selective cathepsin-S inhibitors containing different central cyclic scaffolds. *J Med Chem.* 2013;56(23):9789-9801. <https://doi.org/10.1021/jm401528k>
- Tato M, Kumar SV, Liu Y, et al. Cathepsin S inhibition combines control of systemic and peripheral pathomechanisms of autoimmune tissue injury. *Nat Sci Rep.* 2017;7(1):2775. <https://doi.org/10.1038/s41598-017-01894-y>
- Theron M, Bentley D, Nagel S, et al. Pharmacodynamic monitoring of RO5459072, a small molecule inhibitor of cathepsin S. *Front Immunol.* 2017;8:806. <https://doi.org/10.3389/fimmu.2017.00806> eCollection 2017

19. Ahn JE, Karlsson MO, Dunne A, Ludden TM. Likelihood based approaches to handling data below the quantification limit using NONMEM VI. *J Pharmacokinet Pharmacodyn*. 2008;35(4):401-421. <https://doi.org/10.1007/s10928-008-9094-4>
20. Graff J, Brinch K, Madsen JL. Gastrointestinal mean transit times in young and middle-aged healthy subjects. *Clin Physiol*. 2001;21(2): 253-259.
21. Chan YK, Kwan AC, Yuen H, et al. Normal colon transit time in healthy Chinese adults in Hong Kong. *J Gastroenterol Hepatol* 2004; 19:1270-1275. *J Gastroenterol Hepatol*. 2004;19(11):1270-1275.
22. Chaussade S, Roche H, Khyari A, Couturier D, Guerre J. Measurement of colonic transit time: description and validation of a new method. *Gastroenterol Clin Biol*. 1986;10(5):385-389.
23. Martelli H, Devroede G, Arhan P, Duguay C, Dornic C, Faverdin C. Some parameters of large bowel motility in normal man. *Gastroenterology*. 1978;75(4):612-618.
24. Tomita R, Igarashi S, Ikeda T, et al. Study of segmental colonic transit time in healthy men. *Hepatogastroenterology*. 2011;58(110-111): 1519-1522. <https://doi.org/10.5754/hge10849>
25. Song BK, Cho KO, Jo Y, Oh JW, Kim YS. Colon transit time according to physical activity level in adults. *J Neurogastroenterol Motil*. 2012; 18(1):64-69. <https://doi.org/10.5056/jnm.2012.18.1.64>
26. Karlsson MO, Beal SL, Sheiner LB. Three new residual error models for population PK/PD analyses. *J Pharmacokinetics Biopharmaceutics*. 1995;23(6):651-672.
27. Tannergren C, Bergendal A, Lennernäs H, Abrahamsson B. Toward an increased understanding of the barriers to colonic drug absorption in humans: Implications for early controlled release candidate assessment. *Mol Pharm*. 2009;6(1):60-73. <https://doi.org/10.1021/mp800261a>
28. Heimbach T, Xia B, Lin TH, He H. Case studies for practical food effect assessments across BCS/BDDCS class compounds using in silico, in vitro, and preclinical in vivo data. *AAPS J*. 2013;15(1):143-158. <https://doi.org/10.1208/s12248-012-9419-5>
29. Augustijns P, Vertzoni M, Reppas C, et al. Unraveling the behavior of oral drug products inside the human gastrointestinal tract using the aspiration technique: History, methodology and applications. *Eur J Pharm Sci*. 2020;155:105517. <https://doi.org/10.1016/j.ejps.2020.105517>
30. Alexander SPH, Fabbro D, Kelly E, et al. CGTP Collaborators, The Concise Guide to Pharmacology 2019/20:Enzymes. *Br J Clin Pharm*. 2019a;176(S1):S297-S396.
31. Alexander SPH, Kelly E, Mathie A, et al. The Concise Guide to Pharmacology 2019/20:Transporters. *Br J Clin Pharm*. 2019b;176(S1): S397-S493.

SUPPORTING INFORMATION

Additional supporting information may be found online in the Supporting Information section at the end of this article.

How to cite this article: Kratochwil NA, Stillhart C, Diack C, Nagel S, Al Kotbi N, Frey N. Population pharmacokinetic analysis of RO5459072, a low water-soluble drug exhibiting complex food–drug interactions. *Brit Jnl Clinical Pharma*. 2021; 87(9):3550–3560. <https://doi.org/10.1111/bcp.14771>